


Antimicrobial activity of tellurium-loaded polymeric fiber meshes

Rupy Kaur Matharu ^{1,2}, Zhalan Charani,¹ Lena Ciric,² Upulitha Eranka Illangakoon,¹ Mohan Edirisinghe¹

¹Department of Mechanical Engineering, University College London, London WC1E 7JE, United Kingdom

²Department of Civil, Environmental and Geomatic Engineering, University College London, London WC1E 7JE, United Kingdom

The authors have no conflicts of interest to declare.

Correspondence to: M. Edirisinghe (E-mail: m.edirisinghe@ucl.ac.uk)

ABSTRACT: A series of poly(methylmethacrylate) solutions loaded with varying concentrations of tellurium particles are prepared and processed into continuous and smooth microfiber meshes. Scanning electron microscopy and energy-dispersive X-ray spectroscopy are used to study the morphology and surface elemental composition of the composite fibers. Fiber diameters range between 7 and 14 μm with surface nanopores on the fibers ranging between 100 and 200 nm. Energy-dispersive X-ray spectroscopy confirmed successful incorporation of tellurium particles into the fibers. The concentration of tellurium in the composite significantly influenced fiber diameter, pore size, and morphology. The antibacterial activity of the prepared fibers is tested using *Escherichia coli* K12. The fibers are incubated in bacterial suspensions for 24 h at 37 °C and 150 rpm. Antibacterial activity is assessed through the colony-counting method and is found to be dose dependent. The fibers with 4 wt % tellurium exhibited the most potent antibacterial properties as a 1.16 log reduction was observed. © 2018 Wiley Periodicals, Inc. *J. Appl. Polym. Sci.* **2018**, *135*, 46368.

KEYWORDS: biomedical applications; fibers; manufacturing

Received 19 December 2017; accepted 15 January 2018

DOI: 10.1002/app.46368

INTRODUCTION

Complications related to infectious diseases caused by opportunistic pathogens, such as *Escherichia coli*, *Staphylococcus aureus*, and *Candida albicans*, have significantly decreased due to the availability and use of a wide variety of antibiotics and antimicrobial agents.¹ However, excessive use of these antimicrobials has given rise to a number of drug-resistant pathogens. These microorganisms threaten the effective prevention and treatment of an ever-increasing range of infections, resulting in prolonged illness, disability, morbidity, and mortality.^{2,3} In turn, antimicrobial resistance presents an economic burden on global healthcare, with the cost of treatment for patients with resistant infections being higher than care for patients with nonresistant infections due to longer duration of illness, additional tests, and use of more expensive drugs.^{2,3} Without effective antimicrobials for prevention and treatment of infections, medical procedures become high risk. Alternative approaches to treating antimicrobial-resistant microorganisms are urgently needed.

Bioactive agents such as tetracycline and ampicillin have commonly been used to kill or slow the growth of bacteria. However, because of their broad and often inappropriate use, bacterial resistance to antibacterial drugs has occurred.^{4,5}

Moreover, administration of high-dose antibiotics may also cause adverse side effects and intolerable toxicity. The immobilization of novel antimicrobial particles in polymeric fibers is a relatively recent advancement in antimicrobial materials that may have the potential to aid in the eradication of such infections.^{6,7} The advantages of these fibers are related to their high ratio of surface area to volume and the potential to carry and steadily release a variety of embedded compounds or elements.

Throughout history, various metals have been studied for their antimicrobial properties, in particular silver and copper.⁸ Tellurium (Te) is a metalloid that belongs to the group of chalcogens and was first discovered by Transylvanian chemist Franz-Joseph Mueller in 1782, who was studying gold-containing ores.⁹ Te is a rare element (average content in soil is 0.027 ppm) and is present in various oxidative states. In the environment, Te exists in its elemental form (Te^0) and in inorganic telluride (Te^{2-}), tellurite (TeO_3^{2-}), tellurate (TeO_4^{2-}), and organic dimethyl telluride (CH_3TeCH_3).¹⁰ Te forms various compounds with other metals such as silver and gold.¹¹ Silver ammonium tellurite and potassium iodotellurite were used as antibacterial agents even before the discovery of antibiotics.¹² At physiological pH, Te is

© 2018 The Authors. *Journal of Applied Polymer Science* Published by Wiley Periodicals, Inc.

This is an open access article under the terms of the Creative Commons Attribution License, which permits use, distribution and reproduction in any medium, provided the original work is properly cited.

Table I. Fiber Diameter and Pore Diameter of Te-Loaded PMMA Fiber Meshes

Te loading (wt %)	Fiber diameter (μm)	Pore diameter (nm)
0	7.06 ± 3.77	195 ± 63
1	7.95 ± 4.75	196 ± 81
2	13.7 ± 5.31	102 ± 83
4	13.9 ± 7.05	150 ± 142

mostly found as tellurite and has significant toxicity to bacteria at very low concentrations of $1 \mu\text{g/mL}$.^{13,14}

In 1932, Fleming^{15,16} compared the antibacterial activities of penicillin and tellurite, and in all cases, penicillin-sensitive bacteria were also sensitive to tellurite. Intramuscular injection of a suspension of Te^0 in glucose was used to treat human syphilis; however, one substantial drawback was an intense garlic odor in the patients' breath and urine.¹⁷ Tellurium oxides were used as antimicrobial agents against diseases such as leprosy and tuberculosis before the development of penicillin.¹⁸ Tellurite acted synergistically with the antibiotic cefotaxime when tested on antibiotic-resistant *E. coli*.¹⁹ Therefore, tellurite can be used as an adjuvant for several multiresistant pathogens. Some strains of bacteria may have evolved resistance to tellurium during its historical medical use²⁰ or after its use in the mining and electronics industries increased its presence in the environment.

In recent years, tellurium particles have gained interest as potential antibacterial agents.^{21–25} Zonaro *et al.*²⁵ demonstrated the antibacterial and biofilm eradication activity of Te nanoparticles against *E. coli*, *Pseudomonas aeruginosa*, and *S. aureus*. Pugin *et al.*²⁶ reported Te-containing nanostructures showed the interesting ability to inhibit *E. coli* colonization, but with no apparent cytotoxicity against eukaryotic cells. Carbon fibers coated with Te and Te-Au nanowires have been proposed as precursors of future antimicrobial clothing.²⁷ The organic tellurium IV compound ammonium trichloro(dioxoethylene-*O,O'*-)tellurate, AS101, was reported to inhibit the growth of antibiotic-resistant *Klebsiella pneumoniae*.²⁸

The objective of this research was to fabricate a series of tellurium-loaded polymeric fibers and fiber meshes. The synthesized fibers were characterized by scanning electron microscopy and energy-dispersive X-ray spectroscopy. The antimicrobial properties of the composite fibers were tested especially against *E. coli* strain K12.

EXPERIMENTAL

Materials

Tellurium powder (CAS number 13494-80-9, catalog number 266418, 200 mesh), poly(methyl methacrylate) (PMMA, molecular weight $\sim 120,000$ by gel permeation chromatography), chloroform, Luria Broth (LB), and phosphate-buffered saline (PBS) broth were purchased from Sigma Aldrich (Dorset, England). LB agar was sourced from Invitrogen (ThermoFisher, Paisley, UK). All solvents and chemicals were of analytical grade and used without any purification. *Escherichia coli* K12, *Pseudomonas aeruginosa*, and *Staphylococcus aureus* were used to assess the antibacterial properties of the fibers.

Methods

Polymer Solution Preparation. Tellurium-loaded PMMA solution was prepared in a two-step procedure. First, a 20% w/v polymer solution was prepared in an airtight glass vial by dissolving 8.00 g of PMMA in 40.0 mL of chloroform. The mixture was placed on a magnetic stirrer for 24 h to completely dissolve the polymer. Following this, appropriate quantities of Te powder were suspended in 20.0 mL batches of the PMMA/chloroform solution and left to stir on a magnetic stirrer for 24 h in order to achieve a homogenous dispersion. The weight percent of Te in each fiber batch is shown in Table I.

Fiber Production. Ultrafine fibers were produced using pressurized gyration. To begin, 5 mL of the polymer solution was injected at once using a syringe into the port of the gyrotor. The gyrotor was then switched on and reached a maximum speed of 36,000 rpm to which 0.1 MPa pressure was applied. Further details on the process and related forming videos have been described in previous literature.²⁹ The resulting fibers were deposited on the collector positioned 10 cm away from the gyrotor and were collected and stored in plastic petri dishes.

Fiber Characterization. The obtained fibers were analyzed using a scanning electron microscope (SEM) Quanta 200F (Dartford, UK) with a field-emission gun. To visualize the fibers, the samples were coated with gold in a sputter coater. All of the SEM images were taken at an acceleration voltage of 5 kV. The average fiber diameter was determined by measuring the diameter of all fibers in available images using ImageJ software (National Institutes of Health, Maryland, USA) with DiameterJ plugin.

Energy-dispersive X-ray spectroscopy (EDX) was carried out using an INCA X-Sight (Oxford Instruments, High Wycombe, UK). The voltage used was 20 kV and the working distance was 10 mm. INCA software was used to analyze the EDX spectra.

Antimicrobial Properties. In order to assess the antibacterial activity of Te, the agar diffusion assay was employed. LB agar plates were prepared per manufacturer's instructions and sterilized under ultraviolet light for 4 h. A single colony of *E. coli* was suspended in 500 μL of sterile distilled water in a 1 mL Eppendorf tube. The suspension was then spread onto an LB agar plate using a plastic L-shaped spreader. This was repeated for each bacterium (*P. aeruginosa* and *S. aureus*). Then 10 mg of Te powder was placed on the surface of each inoculated plate using a sterile metal spatula. After application, it was ensured that the powder had made complete contact with the agar surface. The plates were then incubated at 37 °C for 24 h. The assay was performed in triplicate for each bacterial strain. Antibacterial activity was assessed by the diameter of the growth-inhibition zone.

Bacterial cell preparation was carried out as follows. *E. coli* suspensions were grown in 50 mL centrifuge tubes by inoculating 30 mL of sterile LB broth with a single colony using a sterile plastic inoculating loop. The suspensions were cultured at 37 °C and 150 rpm until they reached their midexponential phase (approximately 3 h, $\text{OD}_{600} \sim 0.147$). The cultures were centrifuged at 4600 rpm for 15 min to pellet cells, and the supernatant was discarded. The cells were washed with 20 mL of sterile PBS solution and resuspended in 3 mL of PBS solution. In order to

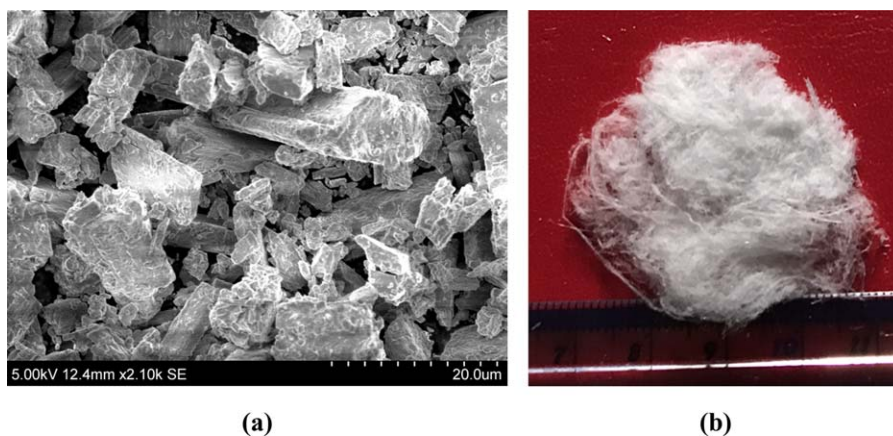


Figure 1. (a) SEM image of the tellurium powder as received; (b) macroscopic image of the 4 wt % tellurium-loaded PMMA fiber mesh. [Color figure can be viewed at wileyonlinelibrary.com]

calculate an approximate concentration of cells in the culture, the colony-counting method was used. This was achieved by performing a series of 10-fold dilutions. Then 50 μL of the dilutions was transferred to individual LB agar plates and incubated at 37 $^{\circ}\text{C}$ for 24 h, after which time the colonies were counted.

To prepare fiber mats, the fibers were cut into 1 cm round disks each weighing approximately 0.02 g. They were then sterilized under ultraviolet light for 1 h.

Cell viability testing was conducted as follows. In a six-well plate, the *E. coli* K12 culture aliquots were placed into each well, and the fiber samples were added. Pure PMMA fibers were used as the negative control. The six-well plate and its contents were incubated for 24 h at 37 $^{\circ}\text{C}$ and 150 rpm. The loss of viability of *E. coli* K12 cells was evaluated by the colony-counting method (as described in the paragraph on bacterial cell preparation). Colonies were counted and compared with those on control plates to calculate changes in the cell growth caused by the presence of Te-loaded fibers. All experiments were performed in triplicate on three separate occasions.

RESULTS AND DISCUSSION

Tellurium Particle Characteristics

SEM images of the Te powder showed the particles to be mainly polygonal [Figure 1(a)]. Although some particle agglomeration was observed, with evidence of clusters $\sim 20\ \mu\text{m}$ in diameter, overall, the size analysis showed particle diameters ranged between 2 and 12 μm .

Fiber Morphology

In this study, PMMA fibers with 1, 2, and 4 wt % Te particles embedded into their matrix were successfully prepared through pressurized gyration. SEM images of these fibers are shown in Figure 2. In all instances, the fibers formed were smooth, continuous, and bead-free with circular surface pores, despite their Te loading. This indicated that the intermolecular entanglement and chain overlap in the solutions were optimal to stabilize the polymer jet and create an adequate Rayleigh–Taylor instability for fiber formation. The formation of continuous fibers suggests the chain entanglement was complete enough to hinder molecular motion and the viscoelastic stresses were strong enough to

stabilize the jet to prevent fiber fracture typically caused by the centrifugal force and pressure difference at the orifice. This also confirms that the presence of Te particles in the polymer solution did not interfere with chain entanglement.

The fiber diameter of PMMA fibers with no Te particles was $7.06 \pm 3.77\ \mu\text{m}$. Increasing the concentration of Te particles from 1 wt % to 4 wt % led to the formation of thicker fibers with a wider diameter distribution (Table I). This observation suggests that the introduction of excess Te particles causes the solution to have a greater resistance against the stretching caused by the forces on the polymer jet. Previous studies²⁹ suggest that a change in fiber diameter in pressurized gyration is the result of a combined effect of polymer concentration, rotational speed, and working pressure although flow into the vessel can also be controlled. However, during this experiment, all of these parameters were kept constant, therefore suggesting Te loading to be the underlying cause. Furthermore, as the Te particles are relatively large in diameter, it can be hypothesized that the presence of Te consequently significantly increases fiber diameter.

High-magnification SEM images of the fiber samples (Figure 3) show nanopores on the surface of all fabricated fibers. The pore diameters ranged between 195 ± 63 and $150 \pm 142\ \text{nm}$ and have been tabulated in Table I. Pore diameter in each of the fiber samples varies in a manner similar to the fiber diameter. Higher Te loading resulted in smaller pore sizes, but the pore diameter variation is higher compared to the fibers with lower Te loading. The surface topography varies hugely as the concentration of Te particles increases. At lower concentrations (0, 1, and 2 wt %), the pores are relatively circular and regularly distributed along the fiber. At 4 wt %, the pores become more irregular and inconsistent in shape, size, and distribution. The generation of surface pores can be explained through solvent volatility, phase separation, and breath figure formation.^{30,31} When the solvent (chloroform) evaporates from the polymer jet, the temperature at the air–liquid interface will decrease rapidly due to the enthalpy of vaporization.³² It was previously reported³³ that the temperature of a chloroform solution can fall between -6 to $0\ ^{\circ}\text{C}$ during evaporation. This temperature drop significantly lowers the dew point of the atmosphere. Due to this effect,

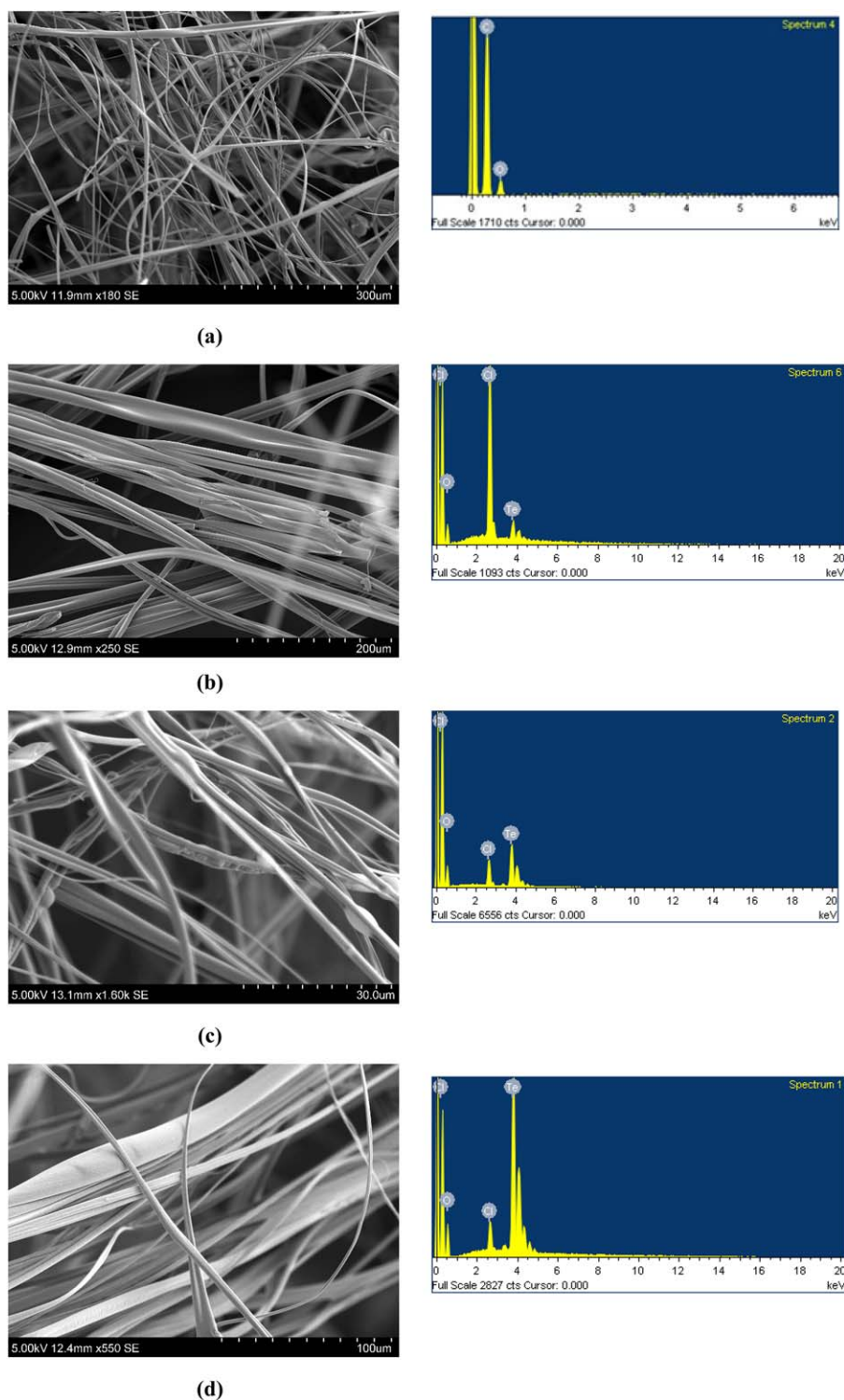


Figure 2. SEM images and EDX spectra of (a) pure PMMA fibers, (b) PMMA fibers with 1.0 wt % tellurium, (c) PMMA fibers with 2.0 wt % tellurium, and (d) PMMA fibers with 4.0 wt % tellurium. [Color figure can be viewed at wileyonlinelibrary.com]

water vapor condenses on the fiber surface. As chloroform is immiscible with water, this limits the penetration of the water droplets into the fiber core. When the water droplets evaporate from the fibers, their imprints remain as pores on the fibers.^{34,35} EDX imaging was used to show that Te was successfully incorporated into the fiber matrix (Figure 2).

Antibacterial Activity

Antibacterial Activity of Tellurium Particles. The agar diffusion assay is a rapid and simple technique used to assess the susceptibility of Gram-positive (*S. aureus*) and Gram-negative (*E. coli*, *P. aeruginosa*) bacteria to antimicrobial agents. In this investigation, the agar diffusion assay was employed to quantify

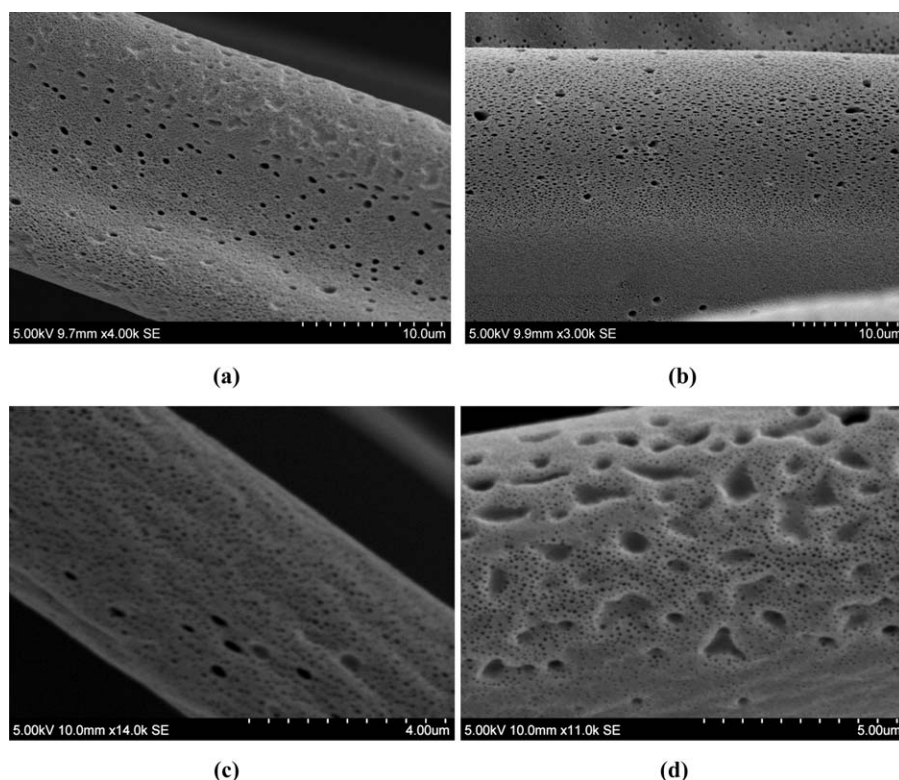


Figure 3. High-magnification SEM images of the fiber surfaces: (a) pure PMMA fibers, (b) PMMA fibers with 1.0 wt % tellurium, (c) PMMA fibers with 2.0 wt % tellurium, (d) PMMA fibers with 4.0 wt % tellurium.

the ability of Te to inhibit bacterial growth. The assay is based on the diffusion of Te from areas of high concentrations to areas of low concentration (the bacteria lawn on the agar surface). From the results displayed in Table II, it can be seen that Te prevented the growth of the Gram-negative bacteria tested, while it has no effect on the Gram-positive bacteria. *E. coli* demonstrated the largest inhibition zone, followed by *P. aeruginosa* and *S. aureus*. The presence of a growth-inhibition zone was interpreted as an antimicrobial effect on the microorganism. Gram-negative bacteria (*E. coli* and *P. aeruginosa*) possess a thin peptidoglycan layer and an outer lipopolysaccharide membrane, whereas Gram-positive bacteria (*S. aureus*) possess a thick peptidoglycan layer and no outer lipopolysaccharide membrane.³⁶ Therefore, in this instance, it can be assumed the thick peptidoglycan layer served as a barrier resistant to the Te particles, as no inhibition was observed with *S. aureus*. From this assay, it can be concluded that Te has a potent ability to inhibit *E. coli* growth, so *E. coli* was selected as the model organism to assess the antibacterial properties of the Te-loaded fibers.

Table II. Zones of Bacterial Growth Inhibition Produced by 10 mg of Tellurium Powder

Bacterial strain	Average growth inhibition zone diameter \pm standard deviation (cm)
<i>P. aeruginosa</i>	0.47 ± 0.15
<i>S. aureus</i>	0.00 ± 0.00
<i>E. coli</i>	1.87 ± 0.32

Antibacterial Activity of Tellurium-Loaded Fiber Meshes. The antibacterial activity of the composite fibers was tested against a representative Gram-negative organism, an important hospital-acquired pathogen. Figures 4 and 5 show the antimicrobial activity of the fibers against *E. coli*. After 24 h of incubation, the control sample showed low cytotoxicity with an average log reduction of 0.03 ± 0.01 . From the results presented here, it can be concluded that Te-loaded fibers exhibit inhibitory activity toward *E. coli*. The antibacterial properties of Te fibers are evidently dose dependent, as a clear positive correlation between Te loading and log reduction can be observed. When increasing the tellurium loading to 1 wt %, a dramatic increase in log reduction in bacterial numbers can be observed. This trend continues as the concentration of Te increases further, until a

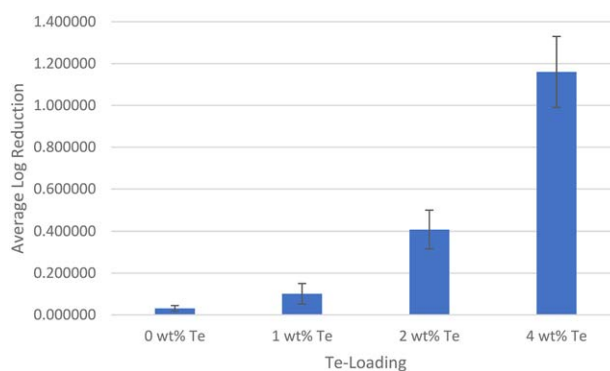


Figure 4. Bacterial growth reduction after treatment with Te-loaded fiber meshes. [Color figure can be viewed at wileyonlinelibrary.com]

maximum log reduction of 1.16 ± 0.17 is observed at 4 wt %. This observed loss of cell viability is considered significant when compared to the control fibers.

Comparing these results to those obtained with fibers loaded with silver nanoparticles (≈ 4 log reduction in bacterial numbers), Te-loaded fibers show a lower log reduction.³⁷ However, it is important to remember the numerous detrimental side effects avoided by bypassing the use of silver nanoparticles in toxic concentrations. Increased exposure to silver nanoparticles carries dangerous environmental and health implications. Side effects of these substances include acute respiratory irritation, caustic injury of the upper gastrointestinal tract or subcutaneous tissue, psychological disorders, and argyria.³⁸ Furthermore, increased concentrations of silver ions (colloids) in the bloodstream of childbearing women have been linked to the development of congenital craniofacial abnormalities in their offspring.³⁸ Te/PMMA composite fibers showed a bactericidal activity similar to zinc oxide/cellulose nanocomposites as well as copper/cellulose nanocomposites, where a maximum 2 log bacterial reduction was achieved.^{39,40} It can be deemed advantageous that the Te/PMMA microscale fibers achieved bacterial log reductions similar to existing nanoparticles, therefore avoiding the use of expensive nanoparticles that are costlier to produce and process.

A multitude of mechanisms can be attributed to the antimicrobial activity of these fibers. One possible mechanism is that Te particles can diffuse through the bacterial cell membrane and cause damage to cellular components by production of reactive

oxygen species, leading to inhibition of enzyme activity and DNA synthesis and disrupting energy transduction.⁴¹ It can also be speculated that bacterial species such as *Bacillus Sp.* can reduce tellurite ions leached from the polymer into the surrounding bacterial solution to elemental Te⁰, thus making nanoparticles.²³ Reduction of these ions is thought to occur through the action of a plasma membrane flavine-dependent reductase. Elemental Te⁰ is insoluble, and accumulation of this material within cells results in potent bactericidal activity, which is demonstrated with kills achieved via a combination of various mechanisms.¹¹ As the fibers were smooth, it cannot be said that the direct physical penetration of Te particles into the bacteria cells is the cause of the observed cytotoxicity.

In this paper, we have achieved significant antibacterial activity without the need for alteration of additional environmental conditions, such as ultraviolet light. Moreover, the composite in this study has the advantage of being cost effective and easy to prepare and is more stable than existing antimicrobial agents. The data presented demonstrate the promising bactericidal properties Te/PMMA fibers have against *E. coli* K12.

CONCLUSIONS

Effective incorporation of Te into the PMMA fibers was confirmed by EDX analysis. The antibacterial activity of the pure Te powder was initially tested using *P. aeruginosa*, *S. aureus*, and *E. coli* using the agar diffusion assay. It was found that pure Te shows the highest antibacterial activity against *E. coli*. For this reason, the antibacterial properties of Te/PMMA composite fibers were tested on *E. coli*. The Te/PMMA fiber meshes show remarkable dose-dependent antibacterial activity toward Gram-negative *E. coli* cells. The bactericidal activity of Te/PMMA fibers reported here is comparable to the results obtained with similar well-established metallic antimicrobial agents, and these meshes can make a significant impact on global health.

ACKNOWLEDGMENTS

The authors would like to thank Dr. Tom Gregory (University College London, Department of Archaeology) for assistance with SEM and EDX microscopy. This work was supported by the UK Engineering and Physical Sciences Research Council (grant EP/N0342281). Data supporting this study are provided in the paper.

REFERENCES

1. Harriott, M. M.; Noverr, M. C. *Antimicrob. Agents Chemother.* **2009**, *53*, 3914.
2. De Kraker, M. E. A.; Wolkewitz, M.; Davey, P. G.; Koller, W.; Berger, J.; Nagler, J.; Icket, C.; Kalenic, S.; Horvatic, J.; Seifert, H.; Kaasch, A.; Paniara, O.; Argyropoulou, A.; Bompola, M.; Smyth, E.; Skally, M.; Raglio, A.; Dumpis, U.; Melbarde Kelmere, A.; Borg, M.; Xuereb, D.; Ghita, M. C.; Noble, M.; Kolman, J.; Grabljevec, S.; Turner, D.; Lansbury, L.; Grundmann, H. J. *Antimicrob. Chemother.* **2010**, *66*, 398.
3. Woolhouse, M.; Waugh, C.; Perry, M. R.; Nair, H. J. *Global Health* **2016**, DOI: 10.7189/jogh.06.010306.
4. Brown, E. D.; Wright, G. D. *Nature* **2016**, *529*, 336.

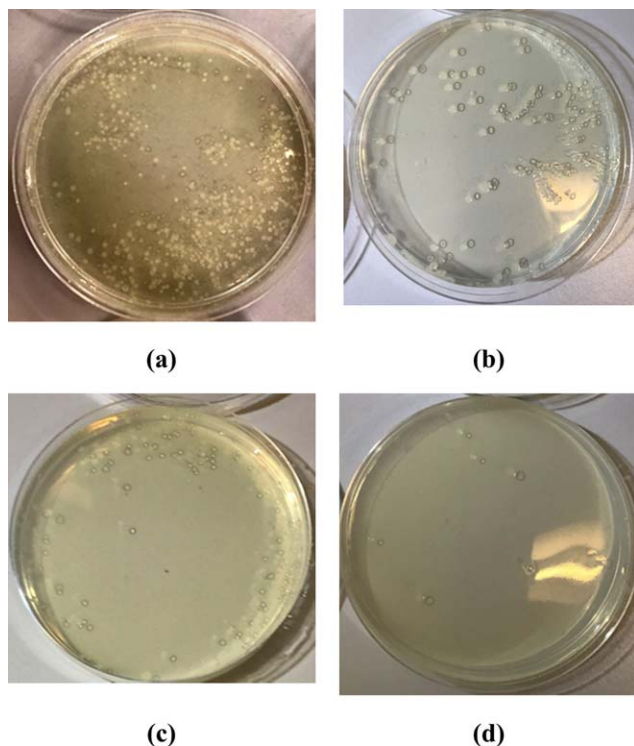


Figure 5. LB agar plates with *E. coli* bacterial growth after 24 h of incubation with (a) 0, (b) 1, (c) 2, and (d) 4 wt % of tellurium-loaded fiber meshes. [Color figure can be viewed at wileyonlinelibrary.com]

5. Walsh, C. *Nature* **2000**, *406*, 775.
6. Allison, S.; Ahumada, M.; Andronic, C.; McNeill, B.; Variola, F.; Griffith, M.; Ruel, M.; Hamel, V.; Liang, W.; Suuronen, E. J.; Alarcon, E. I. *J. Mater. Chem. B* **2017**, *5*, 2402.
7. Agarajan, S.; Soussan, L.; Bechelany, M.; Teyssier, C.; Cavaillès, V.; Pochat-Bohatier, C.; Miele, P.; Kalkura, N.; Janot, J. M.; Balme, S. *J. Mater. Chem. B* **2016**, *4*, 1134.
8. Lemire, J. A.; Harrison, J. J.; Turner, R. J. *Nature Rev. Microbiol.* **2013**, *11*, 371.
9. Ba, L. A.; Doring, M.; Jamier, V.; Jacob, C. *Org. Biomol. Chem.* **2010**, *8*, 4203.
10. Cunha, R. L. O. R.; Gouvea, I. E.; Juliano, L. *An. Acad. Bras. Ciênc.* **2009**, *81*, 393.
11. Zannoni, D.; Borsetti, F.; Harrison, J. J.; Turner, R. J. *Adv. Microb. Physiol.* **2007**, *53*, 1.
12. Chasteen, T. G.; Fuentes, D. E.; Tantalean, J. C.; Vasquez, C. C. *FEMS Microbiol. Rev.* **2009**, *33*, 820.
13. Turner, R. J.; Borghese, R.; Zannoni, D. *Biotechnol. Adv.* **2012**, *30*, 954.
14. Taylor, D. E. *Trends Microbiol.* **1999**, *7*, 111.
15. Fleming, A. *J. Pathology and Bacteriology* **1932**, *35*, 831.
16. Fleming, A.; Young, M. Y. *J. Pathol. Bacteriol.* **1940**, *51*, 29.
17. Frazer, A. D. *Lancet* **1920**, *2*, 133.
18. Demeio, R. H.; Henriques, F. C. J. R. *J. Biol. Chem.* **1947**, *169*, 609.
19. Molina-Quiroz, R. C.; Muñoz-Villagran, C. M.; De La Torre, E.; Tantalean, J. C.; Vasquez, C. C.; Perez-Donoso, J. M. *PLOS One* **2012**, DOI: 10.1371/journal.pone.0035452.
20. Taylor, D. E. *Trends Microbiol.* **1999**, *7*, 111.
21. Chang, H. Y.; Cang, J. S.; Roy, P.; Chang, H. T.; Huang, Y. C.; Huang, C. C. *ACS Appl. Mater. Interfaces* **2014**, *6*, 8305.
22. Lin, Z. H.; Lee, C. H.; Chang, H. Y.; Chang, H. T. *Chem. - Asian J.* **2012**, *7*, 930.
23. Zare, B.; Faramarzi, M. A.; Sepehrizadeh, Z.; Shakibaie, M.; Rezaie, S.; Shahverdi, A. R. *Mater. Res. Bull.* **2012**, *47*, 3719.
24. Zhong, C. L.; Qin, B. Y.; Xie, X. Y.; Bai, Y. *J. Nano Res.* **2013**, *25*, 8.
25. Zonaro, E.; Lampisl, S.; Tumer, R. J.; Qazi, S. J. S.; Vallini, G. *Front. Microbiol.* **2015**, DOI: 10.3389/fmicb.2015.00584.
26. Pugin, B.; Cornejo, F. A.; Muñoz-Díaz, P.; Muñoz-Villagran, C. M.; Vargas-Perez, J. I.; Arenas, F. A.; Vasquez, C. C. *Appl. Environ. Microbiol.* **2014**, *80*, 7061.
27. Chou, T. M.; Ke, Y. Y.; Tsao, Y. H.; Li, Y. C.; Lin, Z. H. *Int. J. Environ. Res. Public Health* **2016**, DOI: 10.3390/ijerph13020202.
28. Daniel-Hoffmann, M.; Albeck, M.; Sredni, B.; Nitzan, Y. *Arch. Microbiol.* **2009**, *191*, 631.
29. Hong, X.; Mahalingam, S.; Edirisinghe, M. *Macromol. Mater. Eng.* **2017**, *302*, 1600564.
30. Yazgan, G.; Dmitriev, R. I.; Tyagi, V.; Jenkins, J.; Rotaru, G. M.; Rottmar, M.; Rossi, R. M.; Toncelli, C.; Papkovsky, D. B.; Maniura-Weber, K.; Fortunato, G. *Sci. Rep.* **2017**, *7*, 158.
31. Megelski, S.; Stephens, J. S.; Chase, D. B.; Rabolt, J. F. *Macromolecules* **2002**, *35*, 8456.
32. Illangakoon, U. E.; Mahalingam, S.; Matharu, R. K.; Edirisinghe, M. *Polymers* **2017**, *9*, 508.
33. Chiu, Y. C.; Kuo, C. C.; Lin, C. J.; Chen, W. C. *Soft Matter* **2011**, *7*, 9350.
34. Srinivasarao, M.; Collings, D.; Philips, A.; Patel, S. *Science* **2001**, *292*, 79.
35. Park, M. S.; Kim, J. K. *Langmuir* **2004**, *20*, 5347.
36. Silhavy, T. J.; Kahne, D.; Walker, S. *Cold Spring Harbor Perspect. Biol.* **2010**, *2*(5), a000414.
37. Paladini, F.; Di Franco, C.; Panico, A.; Scamarcio, G.; Sannino, A.; Pollini, M. *Materials* **2016**, *9*(6), 411.
38. Samberg, M.; Oldenburg, S.; Monteiro-Riviere, N. *Environ. Health Perspect.* **2009**, *118*(3), 407.
39. Martins, N. C. T.; Freire, C. S. R.; Neto, C. P.; Silvestre, A. J. D.; Causio, J.; Baldi, G.; Sadocco, P.; Trindade, T. *Colloids Surf., A* **2013**, *417*, 111.
40. Pinto, R. J. B.; Daina, S.; Sadocco, P.; Neto, C. P.; Trindade, T. *BioMed Res. Int.* **2013**, DOI: 10.1155/2013/280512.
41. Chang, H. Y.; Cang, J. S.; Roy, P.; Chang, H. T.; Huang, Y. C.; Huang, C. C. *ACS Appl. Mater. Interfaces* **2014**, *6*, 8305.